

Rheological quantification of the extent of dissolution of ultrahigh molecular weight polyethylene in melt-compounded blends with high density polyethylene

Krishnaroop Chaudhuri, and Ashish K. Lele

Citation: *Journal of Rheology* **64**, 1 (2020); doi: 10.1122/1.5113705

View online: <https://doi.org/10.1122/1.5113705>

View Table of Contents: <https://sor.scitation.org/toc/jor/64/1>

Published by the [The Society of Rheology](#)

ARTICLES YOU MAY BE INTERESTED IN

Rotational motions of repulsive graphene oxide domains in aqueous dispersion during slow shear flow
Journal of Rheology **64**, 29 (2020); <https://doi.org/10.1122/1.5120323>

Multiple droplets formation in ultrathin bridges of rigid rod dispersions
Journal of Rheology **64**, 13 (2020); <https://doi.org/10.1122/1.5115464>

Capillary breakup extensional electrorheometry (CaBEER)
Journal of Rheology **64**, 43 (2020); <https://doi.org/10.1122/1.5116718>

Elongational rheology of polystyrene melts and solutions: Concentration dependence of the interchain tube pressure effect
Journal of Rheology **64**, 95 (2020); <https://doi.org/10.1122/1.5100671>

Capillary breakup extensional magnetorheometry
Journal of Rheology **64**, 55 (2020); <https://doi.org/10.1122/1.5115460>

GO CaBER: Capillary breakup and steady-shear experiments on aqueous graphene oxide (GO) suspensions
Journal of Rheology **64**, 81 (2020); <https://doi.org/10.1122/1.5109016>



The advertisement features a composite image. On the left, a young child in a blue shirt and shorts is sitting on a glowing red laser line that recedes into the distance. In the center, two Anton Paar rheometers are shown. The text 'True powder rheology' is prominently displayed in the upper right. The Anton Paar logo and name are in the bottom right corner. A 'Find out more' button is located at the bottom center.

True powder rheology

 **Anton Paar**

[Find out more](#)



Rheological quantification of the extent of dissolution of ultrahigh molecular weight polyethylene in melt-compounded blends with high density polyethylene

Krishnaroop Chaudhuri^{1,2} and Ashish K. Lele^{2,3}

¹Polymer Science and Engineering Division, CSIR—National Chemical Laboratory, Pune 411008, India

²Academy of Scientific and Innovative Research (AcSIR), CSIR-HRDC Campus, Ghaziabad 201002, India

³Research and Development Center, Reliance Industries Ltd., Reliance Corporate Park, Navi Mumbai 400701, India

(Received 6 June 2019; final revision received 24 October 2019; published 13 November 2019)

Abstract

Melt compounding of ultrahigh molecular weight polyethylene (UHMWPE) with high density polyethylene (HDPE) promises to be an alternative route to prepare bimodal polyethylene grades. However, complete dissolution of UHMWPE in HDPE cannot be guaranteed during melt compounding. Indeed, in an earlier work [K. Chaudhuri *et al.*, *Polym. Eng. Sci.* **59**, 821–829 (2019)], it was shown that a fully entangled UHMWPE did not mix well with commercial HDPE. However, a disentangled UHMWPE (dPE) could be melt-mixed in the same HDPE as evidenced qualitatively by rheological measurements. The present work is focused on quantifying the extent of dissolution of dPE in HDPE. The proposed method involves fitting rheological models for linear viscoelasticity of entangled bimodal blends of polydisperse polymers to dynamic oscillatory shear data and extracting information on the extent of dissolved species. The time-dependent diffusion model of des Cloizeaux is used along with the theory of double reptation (DR) to describe the dynamics of polydisperse homopolymers and also to extract the molecular weight distribution of the UHMWPE sample. A quadratic mixing rule, consistent with the DR model, is used to describe the dynamics of bimodal blends. Melt-mixed dPE/HDPE blends were prepared and characterized for their linear viscoelastic response by frequency sweep tests. The blends showed complex behavior with multiple crossover points, especially for the higher content of dPE. The bimodal model was then fit to the experimental frequency sweep data to determine the only unknown parameter, namely, the extent of dissolved dPE. It was found that a considerable fraction of dPE is dissolved in HDPE during melt compounding. © 2019 The Society of Rheology. <https://doi.org/10.1122/1.5113705>

I. INTRODUCTION

Bimodal blends of polyethylene are used in several niche applications such as in manufacturing lightweight and stronger blow molded containers and high strength pipes [1–7]. Conventional bimodal polyethylene grades are made in multiple reactors [8–10] and contain fractions of low, medium, and very high molecular weight chains ($>10^6$ g/mol), which endow the blend with improved mechanical properties while retaining its processability and versatility [4–6,11]. An alternative methodology to prepare bimodal blends could involve dissolution of small amounts of ultrahigh molecular weight polyethylene (UHMWPE) into high density polyethylene (HDPE) in a “postpolymerization mixing process.” However, the dissolution of UHMWPE into HDPE during any physical mixing process is not easy. Beneficially, the identical chemical nature of the two polyethylenes significantly reduces enthalpic barriers to dissolution of UHMWPE into HDPE. However, there are at least two kinetic barriers for the dissolution process: (i) the high viscosity ratio of UHMWPE to HDPE causes difficulty in dispersion of molten UHMWPE droplets in the HDPE matrix during the compounding process and (ii) the very low diffusion coefficient of UHMWPE chains into the HDPE matrix slows down the molecular mixing process. Consequently, several nonconventional variants of high shear melt blending [12,13] and solution mixing [14,15] processes have been reported recently for preparing UHMWPE-HDPE blends. Many of

these methods require specialized mixing equipment and large residence times in the blender, both of which could be disadvantageous.

It was shown in recent papers [16,17] that the use of “disentangled” UHMWPE (dPE) instead of a commercial well-entangled UHMWPE allows for easier blending of the former with HDPE in a conventional melt compounder in which the mixing times were comparable with residence times in industrial compounding processes. dPE is a metastable state of UHMWPE and is synthesized using specific homogeneous or heterogeneous catalysts such that the long chains in the as-synthesized polymer are in a significantly disentangled state [18–23]. It is likely that the lower viscosity and higher diffusion coefficient of the poorly entangled chains of dPE enable their dissolution in HDPE. However, the tendency of dPE chains to reentangle with themselves in the melt state so as to reach equilibrium can counter the dissolution process. The time required to reach an entangled state depends on the molecular weight of the dPE [21–24]. For dPE of molecular weight of $\sim 4 \times 10^6$ g/mol, such as the one used in the present work, the time to reach equilibrium at typical melt compounding temperatures can be of the order of a few hours. It was shown that dissolution of dPE in HDPE could be achieved in a twin screw corotating micro-compounder well within this time [16]. However, the extent of dissolution was not quantified.

In a melt compounded blend, the dissolved UHMWPE chains are entangled with HDPE chains and consequently

have a significant influence on the melt rheology of the blend. The undissolved UHMWPE chains, on the other hand, have no effect on the melt rheology of the blend [16]. Therefore, in the earlier work on dPE/HDPE blends, dissolution of the long dPE chains in the HDPE matrix was tracked by measuring linear viscoelastic properties of the blend. Specifically, $\tan \delta$ values obtained from dynamic frequency sweeps were used to indicate the dissolution of dPE in HDPE. The lower the $\tan \delta$ value, the greater the extent of dissolution since the long chains increase the storage modulus more than the loss modulus. However, these indications are qualitative. Quantification of the extent of dissolution is important since it would help in optimizing the amount of dPE to be added to the blend under given compounding parameters, or alternatively, it can help in optimizing the compounding parameters to increase the extent of dissolution. The primary purpose of this article is to quantitatively determine the extent of dissolution of dPE in HDPE using experimental linear viscoelastic properties of the blends. This is done by fitting rheological models of linear viscoelasticity of bimodal miscible polymer blends to the experimental oscillatory shear data. By “bimodal miscible polymer blends,” we specifically imply here mixtures of entangled polymers of the same chemical species such as polyethylene, which have very different molar masses. The individual polymers that form the bimodal blends are also polydisperse in nature. Therefore, the rheological models used in this work are based on refinements of theories of entangled polymer dynamics [25–27], which take into account various relaxation mechanisms for polymer chains as well as polydispersity.

Linear relaxation modulus of a miscible blend can be predicted from known relaxation moduli of individual polymeric components of the blend using a mixing rule. While the simplest mixing rule is a linear law [27,28], a more successful mixing rule [29–31] is a quadratic law that is based on the double reptation (DR) concept [30,32]. The DR model accounts for constraint release effects that couple the dynamics of long and short chains in the blend. Several variants of the tube model can be used to describe the underlying relaxation dynamics of individual components of the blend [28]. Recently, it was shown that the time-dependent diffusion (TDD) model by des Cloizeaux [33] better represents the individual chain dynamics in a blend [34,35]. Thus, in this work, the TDD-DR model was used for calculations of linear rheology of blends.

dPE/HDPE blends containing varying quantities of dPE between 1% and 10% by weight were prepared by the melt compounding process. The linear viscoelasticity of individual polymers and their blends was characterized using isothermal small amplitude oscillatory shear (SAOS) measurements. The TDD-DR model was used to fit linear viscoelastic data of individual polymers. In the case of HDPE, the molecular weight distribution (MWD) obtained from the TDD-DR model was validated using independently measured MWD from size exclusion chromatography (SEC). However, the MWD of dPE could not be determined independently due to experimental limitations of SEC. In this case, the rheological technique for determining MWD was first validated using data available in the literature on dPE, following which the

rheological technique was implemented for the dPE used in the present work. Having thus modeled the rheology of individual polymers, the experimental data on blend rheology were fit to the bimodal blends model from which the dissolved weight fraction of dPE was determined.

II. THEORY

A. Polydisperse polymers

Theories for linear viscoelasticity of polydisperse polymers involve a stress relaxation function for individual monodisperse components of the polymer and an appropriate mixing rule. The TDD model by des Cloizeaux [30,33] provides the following expression for stress relaxation function $\mu_s(t, M)$ of an individual monodisperse component of molecular weight M [34]:

$$\mu_s(t, M) = \frac{8}{\pi^2} \sum_{p:\text{odd}} \frac{1}{p^2} \exp(-p^2 U(t)), \quad (1)$$

where

$$U(t) = \frac{t}{\tau_{\text{rept}}} + \frac{1}{H} g\left(\frac{Ht}{\tau_{\text{rept}}}\right). \quad (2)$$

The first term on the right side of Eq. (2) is the relaxation function of the classical Doi and Edwards reptation model. The second term represents contribution to relaxation due to Rouse-like time-dependent diffusive motions of polymers inside renewable tubes formed by other polymer chains; this is akin to tube length fluctuations [36]. The function $g(y)$ can be approximated as $g(y) \approx -y + y^{1/2} [y + (\pi y)^{1/2} + \pi]^{1/2}$. Parameter $H = M/M^*$ can be interpreted as the number of entanglements per chain. M^* is an important parameter of the TDD model. It is an intrinsic material parameter, which is proportional to the entanglement molecular weight M_e , although no universal proportionality has been found [34]. The entanglement molecular weight has the usual definition $M_e = \rho RT/G_N^0$, where ρ is the melt density of the polymer, R is the universal gas constant, and G_N^0 is the plateau modulus [37]. We postulate that since M_e is a function of temperature [38,39], M^* will also vary likewise. The reptation time τ_{rept} is related to the molecular weight M by

$$\tau_{\text{rept}} = KM^3, \quad (3)$$

where the proportionality constant K is the second important parameter of the TDD model.

In a polydisperse polymer, the chains forming the tube are also relaxing of their own accord; therefore, constraint release [28] is a prevalent mechanism of stress relaxation. The effect of constraint release on stress relaxation is captured by the DR concept, which assumes a binary nature of entanglements between neighboring chains and proposes that the relaxation function can be calculated from the single reptation function of Eq. (1) as [40,41]

$$\mu_d(t, M) = \mu_s(t, M)^\beta, \quad (4)$$

where β should be strictly equal to 2. However, some authors [34,42,43] have used slightly higher values for β in their implementation of the DR model, arguing that higher order entanglements or tube dilation account for this deviation [34].

Thus, in the DR model, the relaxation modulus $G(t)$ of a polydisperse linear polymer is given by [30,34,40]

$$G(t) = G_N^0 \left(\int_{\log M_c}^{\infty} (\mu_d(t, M))^{1/\beta} w(M) d \log M \right)^\beta. \quad (5)$$

Here, $w(M) = dW(M)/d \log M$ is the MWD and $W(M)$ is the cumulative weight fraction of chains with a molecular weight less than M . An additional Rouse relaxation term can be added to Eq. (5) [34]. However, in this study, the Rouse

contributions were neither pronounced for the individual polymers nor for their blends. Hence, these contributions were neglected in the present study with minimal loss in accuracy.

B. Bimodal blends

Bimodal blends of polymers of distinctly different molecular weights represent a special case of polydisperse systems in which constraint release couples the dynamics of long and short chains, and the same can be modeled using the DR concept. Following des Cloizeaux [29] and Tsenoglou [41], the relaxation modulus of a bimodal blend of monodisperse polymers can be written as

$$\frac{G_{\text{blend}}(t)}{G_N^0} = \left[\phi_1 \left(\frac{8}{\pi^2} \sum_{p:\text{odd}} \frac{1}{p^2} \exp(-p^2 U_1(t)) \right) + \phi_2 \left(\frac{8}{\pi^2} \sum_{p:\text{odd}} \frac{1}{p^2} \exp(-p^2 U_2(t)) \right) \right]^2. \quad (6)$$

Here, ϕ_1 and ϕ_2 are volume fractions of the two polymers. For bimodal blends of polydisperse polymers such as the ones encountered in this work, namely, dPE and HDPE, Eq. (6) can be rewritten using Eq. (5) as [44]

$$\frac{G_{\text{blend}}(t)}{G_{N,\text{PE}}^0} = \left[x_{\text{dPE}} \int_{\log M_c}^{\infty} \sqrt{\mu_{d,\text{dPE}}(t, M)} w_{\text{dPE}}(M) d \ln M + (1 - x_{\text{dPE}}) \int_{\log M_c}^{\infty} \sqrt{\mu_{d,\text{HDPE}}(t, M)} w_{\text{HDPE}}(M) d \ln M \right]^2. \quad (7)$$

On the right side of Eq. (7), the volume fractions ϕ are replaced by weight fractions x , which assumes that the melt densities of the two polyethylene components are identical. x_{dPE} in Eq. (7) is the weight fraction of “dissolved” dPE in the blend. Note that x_{dPE} will be less than or equal to the amount of dPE added to the formulation. As mentioned earlier, the purpose of this work was in fact to determine x_{dPE} . Furthermore, in Eq. (7), $\mu_{d,\text{dPE}}$ and $\mu_{d,\text{HDPE}}$ are, respectively, the stress relaxation functions of the polydisperse dPE and HDPE components, which can be calculated if their respective TDD parameters K and M^* are known. $w_{\text{dPE}}(M)$ and $w_{\text{HDPE}}(M)$ are, respectively, the molecular weight distributions of the dPE and HDPE components. On the left side of Eq. (7), $G_{N,\text{PE}}^0$ is the molecular weight-independent plateau modulus of polyethylene, which is experimentally determinable and is also documented in the literature [39]. Similarly, $G_{\text{blend}}(t)$ on the left side of Eq. (7) is an experimentally measured quantity. Thus, if the molecular weight distributions of the two individual components are known, then the fraction of dissolved dPE is the only unknown in Eq. (7) and can be obtained by fitting to the experimental data.

Equation (7) should ideally be used for modeling the rheology of bimodal blends whose relaxation spectrum (described by $\mu_{d,\text{dPE}}$ and $\mu_{d,\text{HDPE}}$) does not change with time during the course of rheological measurements. The melt-mixed samples of dPE/HDPE bimodal blends studied in the present work are likely to contain some amounts of undissolved dPE, which can continue to homogenize in HDPE and thereby change the relaxation spectrum during

rheological measurements. However, based on the results of our earlier work [16] wherein the predominant role of shear on dissolution of dPE in HDPE was demonstrated, it can be expected that the extent of dissolution of dPE in HDPE under the near-quiescent conditions during linear viscoelastic measurements is likely to be small compared to the high shear conditions prevalent in a melt-mixing equipment in which the blend was prepared prior to rheological measurements. This was also supported by independent experiments, which showed that when dPE powder was hand-mixed with HDPE pellets and pressed into a disk without melt compounding, hardly any dissolution of dPE was observed in the disk at the end of 30 min of linear viscoelastic measurements. In contrast, when the same amount of dPE powder was first melt-mixed with HDPE in a high shear equipment, then a significant extent of dissolution of dPE was observed. Thus, Eq. (7) is a reasonable approximation for modeling rheology of dPE/HDPE bimodal blends.

C. Generalized exponential function

While high temperature size exclusion chromatography (HT-SEC) was used in the present study to determine absolute MWD of HDPE (see Sec. III), the same was not possible for dPE due to limitations of columns and detectors. Hence, the MWD of dPE was obtained by the rheological technique, which involved the inversion of Eq. (5) and fitting the same to experimental linear viscoelastic data. Following van Ruymbeke *et al.* [35], the generalized exponential (GEX)

function [45,46] was used to determine the MWD of dPE. The GEX function is defined as

$$w_{\text{GEX}}(M) = c \left[\frac{M}{M_0} \right]^{a+1} \exp \left(- \left[\frac{M}{M_0} \right]^b \right). \quad (8)$$

In Eq. (8), a , b , and M_0 are fitting parameters and the constant c is defined as [47]

$$c = \frac{b}{\Gamma \left(\frac{a+1}{b} \right)}. \quad (9)$$

The weight-average molecular weight is then given as

$$M_w = M_0 \frac{\Gamma \left(\frac{a+2}{b} \right)}{\Gamma \left(\frac{a+1}{b} \right)} \quad (10a)$$

and the number average molecular weight is given as

$$M_n = M_0 \frac{\Gamma \left(\frac{a+1}{b} \right)}{\Gamma \left(\frac{a}{b} \right)}. \quad (10b)$$

Thus, for a given set of a , b , and M_0 values, Eq. (8) is the GEX representation of MWD, which was determined in the present work using the following inversion algorithm. Starting from arbitrarily chosen values of a , b , and M_0 , the corresponding $w_{\text{GEX}}(M)$ was calculated using Eq. (8). This was inserted in Eq. (5) along with Eqs. (1)–(4). The calculated relaxation modulus $G(t)$ was then Fourier transformed into the corresponding $G'(\omega)$ and $G''(\omega)$ [48] by using the approximation method of Schwarzl [49]. The calculated storage and loss moduli were compared with the experimental data and the error was minimized using a Nelder–Mead simplex method [50] implemented in MATLAB. The minimization criterion was defined based on relative error $\chi^2 < 2$, where

$$\chi^2 = \frac{1}{2k} \left(\sum_{i=1}^k \frac{[G'_{\text{exp},i} - G'_{\text{mod},i}]^2}{[G'_{\text{exp},i}]^2} + \sum_{i=1}^k \frac{[G''_{\text{exp},i} - G''_{\text{mod},i}]^2}{[G''_{\text{exp},i}]^2} \right). \quad (11)$$

Here, $i = 1, 2, \dots, k$ are the frequency points where the experimental points ($G'_{\text{exp},i}$, $G''_{\text{exp},i}$) and the model fits ($G'_{\text{mod},i}$, $G''_{\text{mod},i}$) are compared. The average molecular weights and polydispersity index ($\text{PDI} = M_w/M_n$) were simultaneously calculated using Eq. (10) at every iteration.

III. EXPERIMENTAL DETAILS

A. Materials

The dPE sample of nominal molecular weight $M_w = 3.5 \times 10^6$ g/mol was supplied by Professor Sanjay Rastogi. Details about the synthesis of dPE are available in the literature [23]. The MWD of dPE was calculated

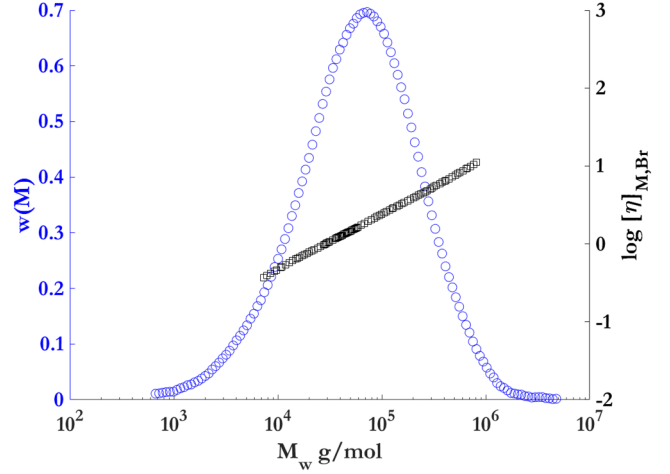


FIG. 1. Absolute MWD of HDPE resin obtained from triple detector HT-SEC. The viscosity-molecular weight data show an exponent of 0.7.

from rheological data as described in Sec. II C. HDPE [melt flow index (MFI) 1.0 g/10 min at 190 °C/2.16 kg] was supplied by Reliance Industries Ltd. The absolute MWD of HDPE was obtained using HT-SEC equipped with three detectors: refractive index, light scattering (right angle and 7° low angle, Malvern Instruments), and viscosity (4 capillary bridge, Viscotek 430). The absolute MWD data for HDPE as obtained from HT-SEC is shown in Fig. 1. The various average molecular weights of the HDPE are $M_n = 17\,236$ g/mol, $M_w = 131\,000$ g/mol, and $M_z = 440\,900$ g/mol. The polydispersity index is 7.6. The viscosity-molecular weight data show a Mark–Houwink exponent of 0.7 over the entire MWD, thereby indicating the linear architecture of the chains with no long chain branching.

B. Blending

Known amounts of HDPE were added through a hopper to a 5 cm³ volume microcompounder (DSM Xplore), having corotating and conical twin screws and a recycle path. The dPE was hand-mixed with excess Irganox 1010 (~1% of the total PE weight to minimize thermooxidative degradation) and was fed into the compounder immediately after the HDPE. The temperature of the melt was set at 190 °C. Based on previous studies [16], the screw speed and mixing time were chosen as 150 rpm and 5 min, respectively. The amounts of dPE added to HDPE was varied from 0% to 10% by weight. The blends were assigned nomenclature as “W_dPE”, where W is the dPE wt. % added to the blend. Extruded strands of the blends were hot compressed into disks of 8 mm diameter at 190 °C and used for rheological measurements.

C. Rheometry

SAOS experiments were performed in the ARES G2 strain-controlled rheometer (TA Instruments) using 8 mm parallel plate geometry. The blends were subjected to a strain of 15%, which was determined to be within the range of linear viscoelasticity from separate strain sweep experiments. The frequency was varied from a maximum value of 600 rad/

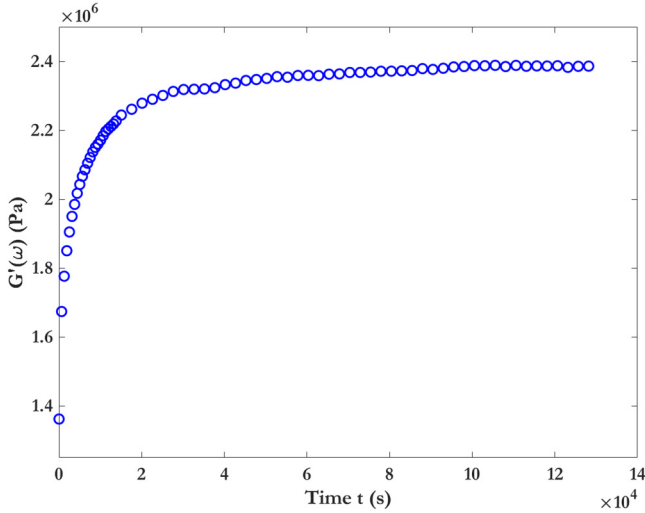


FIG. 2. Time evolution of storage modulus of pure dPE during annealing of the melt at 190 °C using 10 rad/s frequency. The increase in storage modulus reflects an approach to the equilibrated entangled state from an initial metastable disentangled state.

s to a minimum value that was sample dependent. An axial force of 0.05 N was applied on all blend samples throughout the tests to prevent them from slipping between the plates. The temperature of testing was kept at 190 °C using a forced convection oven supplied with nitrogen. To generate SAOS data for the pure dPE, the powders were compacted by hand at room temperature inside a 12-mm mold to form disks of ~ 1 -mm thickness, out of which 8 mm disks were punched out. The inherent disentangled nature of the dPE powders allowed compacting at ambient temperature to be possible. The method is described in our earlier paper [16]. The dPE sample was first subjected to a dynamic time sweep test at 190 °C under nitrogen atmosphere. A constant frequency of 10 rad/s was applied with a strain of 0.5%. Once the elastic modulus reached a saturation value after about 36 h, the SAOS test was performed on the equilibrated sample at a strain amplitude of 0.5% under an axial force of 8 N.

IV. RESULTS AND DISCUSSIONS

A. SAOS data of pure components and blends

Figure 2 shows dynamic time sweep data for pure dPE in which the storage modulus $G'(\omega)$ can be seen to increase rapidly with time during the first 3 h followed by a slower approach to the final equilibrium value, which was achieved after 36 h. This evolution of $G'(\omega)$ is in accordance with earlier reports [21–23], which suggests gradual conversion of the initial metastable disentangled state into an equilibrated well-entangled state. Figure 3(a) shows the SAOS data of the equilibrated dPE, and Fig. 3(b) shows the same for HDPE (0_dPE sample). Over the measured frequency range, the HDPE sample shows dominantly viscous behavior ($G''(\omega) > G'(\omega)$) and a crossover point at high frequency. The scaling exponents of the moduli with frequency are less than the expected values in the terminal regime due to polydispersity effects. Over the same frequency range, the dPE shows predominantly elastic behavior ($G'(\omega) < G''(\omega)$). G' is nearly independent of frequency, while G'' is a decreasing function of frequency; both of which indicate a crossover point at the frequency lower than that probed experimentally. Thus, the nominal relaxation time of dPE (inverse of crossover frequency) is orders of magnitude greater than that of HDPE. This is to be expected based on the difference in their molecular weights and the strong dependence of relaxation time on the molecular weight.

Figure 4 shows the SAOS data for HDPE/dPE blends. For any given frequency over the measured range, both storage and loss moduli increased with an increasing dPE content in the HDPE blends, indicating that the amount of dPE dissolved during melt compounding increases as more dPE was added to the microcompounder. Due to the long relaxation times of dPE chains, the concentration of dissolved dPE affects the low-frequency region more prominently. The high frequencies are mostly dominated by the shorter HDPE chains. In the lower frequency range, the increase in G' was found to be greater than G'' , resulting in the decrease of loss tangent with increasing the dPE content. This result was used in recent works as a qualitative indicator of dissolution of

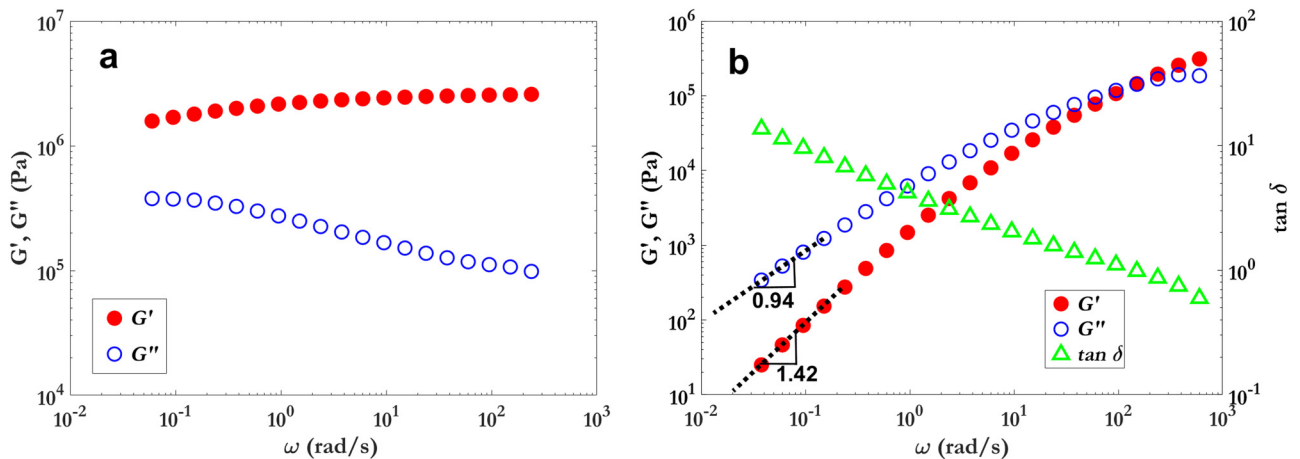


FIG. 3. SAOS data at 190 °C of (a) pure dPE on equilibration after time sweep of 36 h, and (b) pure HDPE; slopes in the low-frequency regions deviate from terminal scaling for monodisperse polymers $G' \sim \omega^2$ and $G'' \sim \omega$, which is indicative of the polydispersity of the sample. The crossover point for HDPE is at $\omega_c \approx 200$ rad/s.

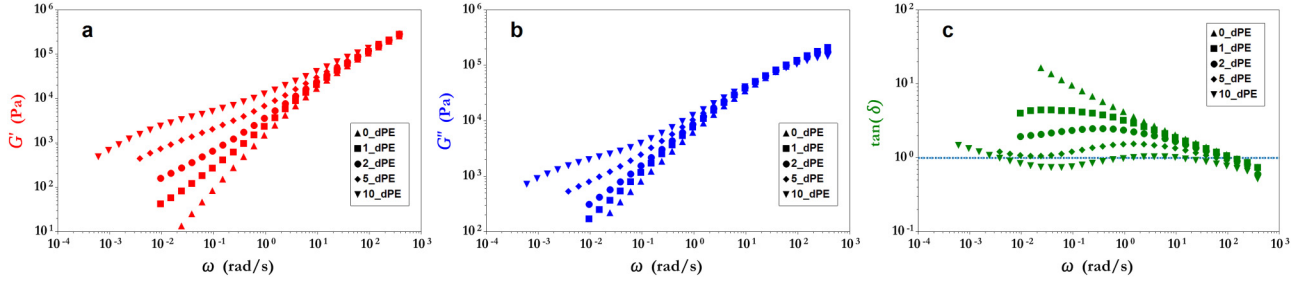


FIG. 4. Comparison of (a) G' , (b) G'' , and (c) $\tan \delta$ of dPE/HDPE blends as a function of the dPE content.

dPE in HDPE [16,17]. The loss tangent of the blends also showed complex nonlinear frequency dependence as the dPE content increased. At the same time, multiple crossover points were seen for blends containing higher dPE content (as indicated by the dashed horizontal line for $\tan \delta = 1$ in Fig. 4). Therefore, in general, the linear viscoelastic frequency sweep data of dPE/HDPE blends showed complex behavior, which naturally provided for a rigorous way to test the model for bimodal blends.

B. Model fitting

Fitting the TDD-DR model for bimodal blends to their experimental SAOS data requires determination of the MWD of dPE. In the absence of independent HT-SEC data for dPE, the SAOS data for an equilibrated sample was used to determine MWD by using the inversion algorithm. Determination of MWD from rheology typically requires SAOS data in the terminal regime [35,51]. However, as shown in Fig. 3(a), the dPE sample shows neither a terminal region nor a crossover point. Therefore, in order to verify the applicability of rheological determination of MWD for dPE the strategy adopted here was to use the inversion algorithm to determine MWD of at least one lower molecular weight dPE sample used by Talebi *et al.* [18] for which the available SAOS data showed a clearly visible crossover point and a small part of the low-frequency regime. Further, independent HT-SEC data are

also available for this dPE sample in Talebi *et al.* [18], which allowed for quantitative comparison between MWDs obtained from the inversion algorithm and HT-SEC.

The inversion of Eq. (5) is an ill-posed problem and requires simultaneous optimization of the five parameters K , M^* , a , b , and M_0 . The likelihood of the regularization function getting trapped in physically unrealistic local minima is high. Consequently, the initial guess values of the parameters often determine the outcome of the regularization problem. Initial guesses for K and M^* for polyethylene were decided based on the available literature; these are $K \sim 10^{-17}$ s(mol/g)³ and $M^* \sim 10\,000 - 30\,000$ [34]. Initial guess values of the other parameters were so chosen as to yield physically realistic solutions. Incorrect choices often resulted in unusually low or high values of M_w than those expected for dPE. The value of G_N^0 for the two dPE samples from Talebi *et al.* [18] was taken to be 2.0 MPa based on values of elastic modulus in the high frequency region of the SAOS data. The results of optimization exercise for these samples are summarized in Table I. The values of K and M^* were found to be close to the numbers reported in the literature. It was found that varying the initial guess values of the parameters a and b by 20% and M_0 by 1000% around those listed in Table I resulted in the same optimized solution. Initial guess values outside this range resulted in unrealistic values of M_w . Figure 5(b) shows the reported MWD obtained from HT-SEC for “Batch No. 1” sample of Talebi *et al.* [18]. Also

TABLE I. Optimized values of model parameters for Talebi *et al.*'s dPE samples and the polyethylene pure components used in the present work. Parameters are obtained from fitting the TDD-DR model with GEX function to SAOS data using the inversion algorithm.

| Sample name | Batch No. 1 ^a | Batch No. 4 ^a | 100_dPE (pure dPE) ^b | 0_dPE (pure HDPE) ^b |
|---|--------------------------|--------------------------|---------------------------------|--------------------------------|
| T (°C) | 160 | 160 | 190 | 190 |
| TDD parameters | | | | |
| K ($\times 10^{-17}$) s(mol/g) ³ | 3.16 | 8.73 | 3 | 0.457 |
| M^* (g/mol) | 20 000 | 20 000 | 36 000 | 36 000 |
| GEX parameters | | | | |
| a | 5.78 | 8 | 1.02 | 1.47 |
| b | 0.78 | 0.58 | 0.37 | 0.23 |
| M_0 (g/mol) | 148 000 | 36 000 | 26 521 | 2.531 |
| Molecular weight distribution | | | | |
| M_w^{expt} (g/mol) | 2.3×10^6 | 4.3×10^6 | — | 131 000 |
| M_w^{GEX} (g/mol) | 2.4×10^6 | 4.2×10^6 | 3.7×10^6 | 132 432 |
| PDI^{exp} | 1.9 | 2.3 | — | 6 |
| PDI^{GEX} | 1.2 | 1.2 | 4.6 | 6.6 |

^adPE samples of Talebi *et al.*

^bPolyethylene pure components used in the present work.

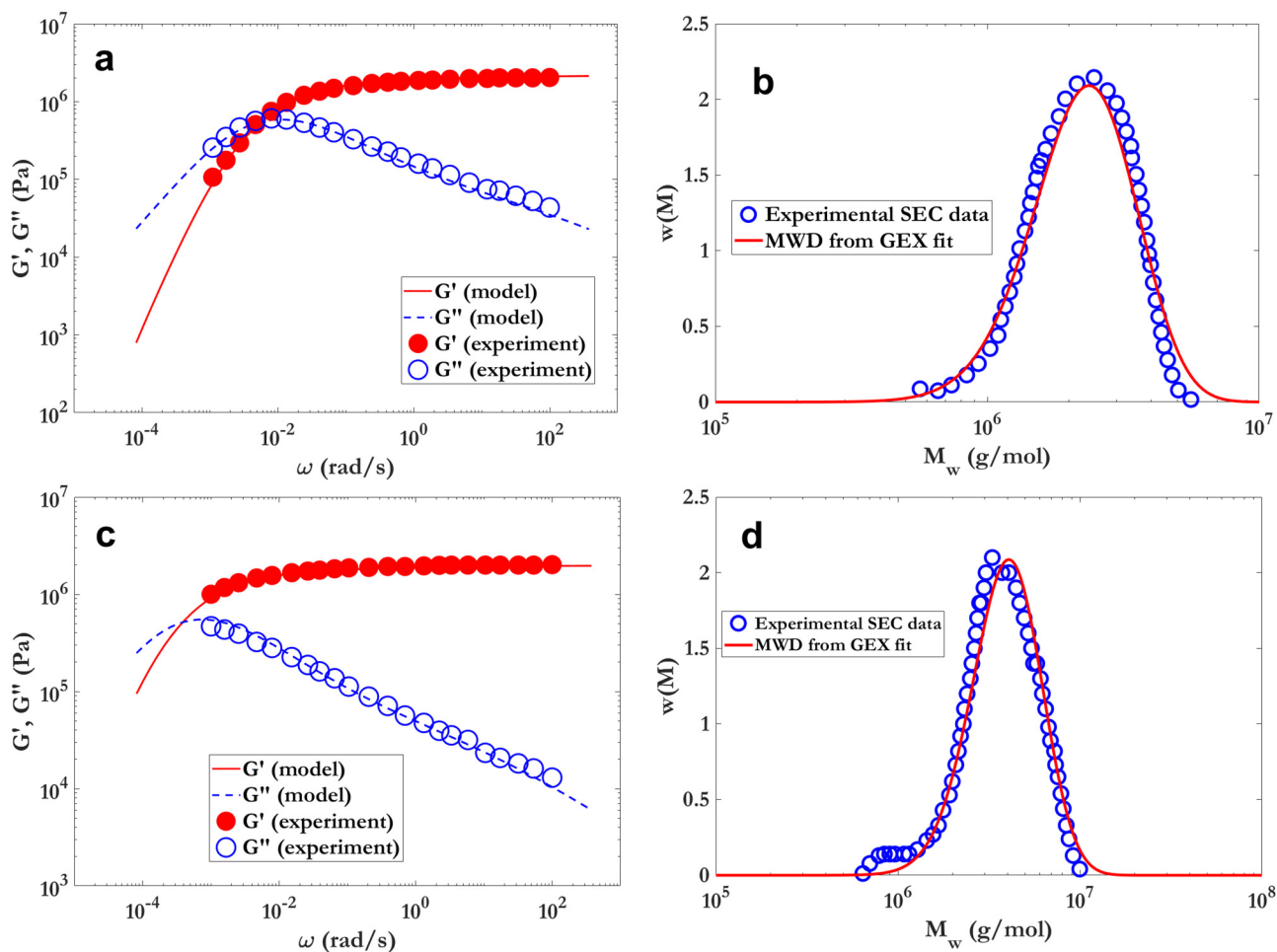


FIG. 5. Results of fitting the TDD-DR + GEX model to the dPE data of Talebi *et al.* [18]. The SAOS fits are shown in (a) for sample “Batch No. 1” and (c) for sample “Batch No. 4.” The resulting MWDs obtained from the inversion algorithm are compared against their respective experimental SEC data in (b) for sample “Batch No. 1” and (d) for sample “Batch No. 4.”

shown in the figure is the MWD as obtained from the inversion algorithm. The comparison between rheologically determined MWD and HT-SEC data was found to be reasonable. The reported MWD measured by HT-SEC was $M_w^{\text{SEC}} = 2.3 \times 10^6$ g/mol with $\text{PDI}^{\text{SEC}} = 1.9$. The inversion algorithm gave $M_w^{\text{GEX}} = 2.4 \times 10^6$ g/mol with $\text{PDI}^{\text{GEX}} = 1.2$.

The same exercise was also repeated for the sample “Batch No. 4” in the paper of Talebi *et al.*, for which $M_w^{\text{SEC}} = 4.3 \times 10^6$ g/mol and $\text{PDI}^{\text{SEC}} = 2.3$. The value of M^* was kept the same as for the Batch No. 1 sample since it is expected to be independent of chain length. However, the other parameters were allowed to be different. As observed from Fig. 5(d), a reasonable fit was obtained for the MWD with $M_w^{\text{GEX}} = 4.2 \times 10^6$ g/mol and $\text{PDI}^{\text{GEX}} = 1.2$. The higher PDI seen experimentally is perhaps a reflection of the small amount of low molecular weight component (peak at $\sim 8 \times 10^5$ g/mol seen in the HT-SEC data), which is not predicted by the inversion of Eq. (5) with GEX distribution. Based on these comparisons, the inversion algorithm was considered to provide acceptable predictions of MWD of dPE from SAOS data for the cases where SEC data of dPE were not available.

The same rheological technique was then applied to the dPE sample used in the present work to determine its MWD.

All five parameters of the combined GEX + TDD-DR model were simultaneously optimized by the inversion algorithm. In Eq. (5), the value of the plateau modulus for the dPE samples used in the present work was taken as $G_N^0 = 2.76$ MPa, which is the value observed in the dynamic oscillatory rheology data for dPE. This is also within the range of reported values for polyethylene [39,52]. Figure 6 shows the MWD predicted by the inversion algorithm. The weight-average molecular weight is calculated to be $M_w = 3.7 \times 10^6$ g/mol, and the PDI was 4.6. The value of the TDD parameters resulting from the optimization were $K_{\text{dPE}} = 3 \times 10^{-17}$ s(mol/g)³ and $M^* = 36000$ g/mol. The value of K_{dPE} is of the same order of magnitude as that for samples of Talebi *et al.* M^* was found to be higher than for Talebi’s samples, which is likely because the temperature of measurement of SAOS data in the present work (190 °C) was higher than that in the work of Talebi *et al.* (160 °C). Since M_e is known to be an increasing function of temperature [39] and since M^* is proportional to M_e , therefore, the higher value of M^* for dPE at 190 °C is considered reasonable. The same value of M^* was used for HDPE in the present work.

As further validation of the applicability of the inversion algorithm, the MWD of HDPE was predicted from its SAOS data and compared with the independently measured

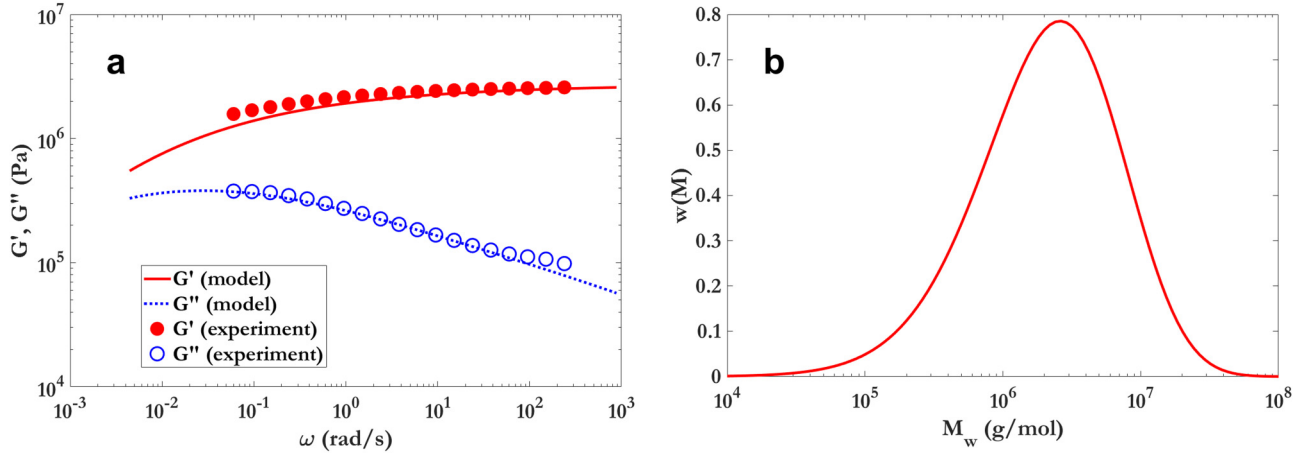


FIG. 6. Results of fitting the TDD-DR + GEX model to the frequency sweep data of equilibrated dPE used in this work. The SAOS fits are shown in (a) and the resulting MWD obtained from the inversion algorithm is shown in (b).

HT-SEC data. The comparison is shown in Fig. 7. The mean squared error between the two plots is only 9%. It is evident that the inversion algorithm predicts the MWD with a reasonable degree of accuracy. The average molecular weights, $M_w^{\text{SEC}} = 131\,000$ g/mol and $M_w^{\text{GEX}} = 132\,342$ g/mol are comparable and so are the polydispersity indices, $\text{PDI}^{\text{SEC}} = 6$ and $\text{PDI}^{\text{GEX}} = 6.6$. The values of the five fit parameters of the inversion algorithm are summarized in Table I for all polyethylene pure components used in this work.

As shown in Table I, while M^* was kept identical for dPE and HDPE, the K values were allowed to be different. This is different from the work of van Ruymbeke *et al.* [34] who used the same value of K for polystyrenes of different molecular weights in order to model the rheology of bidisperse and tridisperse blends prepared using them. In fact, the choice of using the same value of K for dPE and HDPE was also exercised in the present work, but as will be shown later this resulted in poorer model fits for blends. One rationale for using different K values is that there is actually no consensus in the literature about the value of K for a given polymer. For instance, K values for polystyrene (PS) of similar molecular

weights have been reported to be 1.05×10^{-15} s(mol/g)³ [34] and 2.2×10^{-15} s(mol/g)³ [33]. Another reason for allowing K to vary is that while the M^3 dependence in Eq. (1) may be reasonably valid for the melt of very long chains (such as dPE), it is unlikely to hold for the melt of short chains (such as HDPE) or even for blends of short and long chains (such as HDPE/dPE blends). Hence, the variation in values for K might reflect the differences in M^α , where α can vary between 3.0 and 3.4 for the two polyethylenes [53]. In the work of van Ruymbeke *et al.* [34], the molecular weights of polystyrenes were relatively close to each other; the ratio between the weight-average molecular weights of long and short PS chains was ~ 3 . In contrast, the ratio of weight-average molecular weights between dPE and HDPE used in the present work is ~ 30 . Therefore, it is likely that even a tiny fraction of dPE dissolved in the HDPE matrix will drastically alter the relaxation dynamics of the net system. This may necessitate the use of a disparate K values for dPE and HDPE.

The amount of dPE dissolved in HDPE/dPE blends (x_{dPE}) can now be calculated from Eq. (7). The pure component

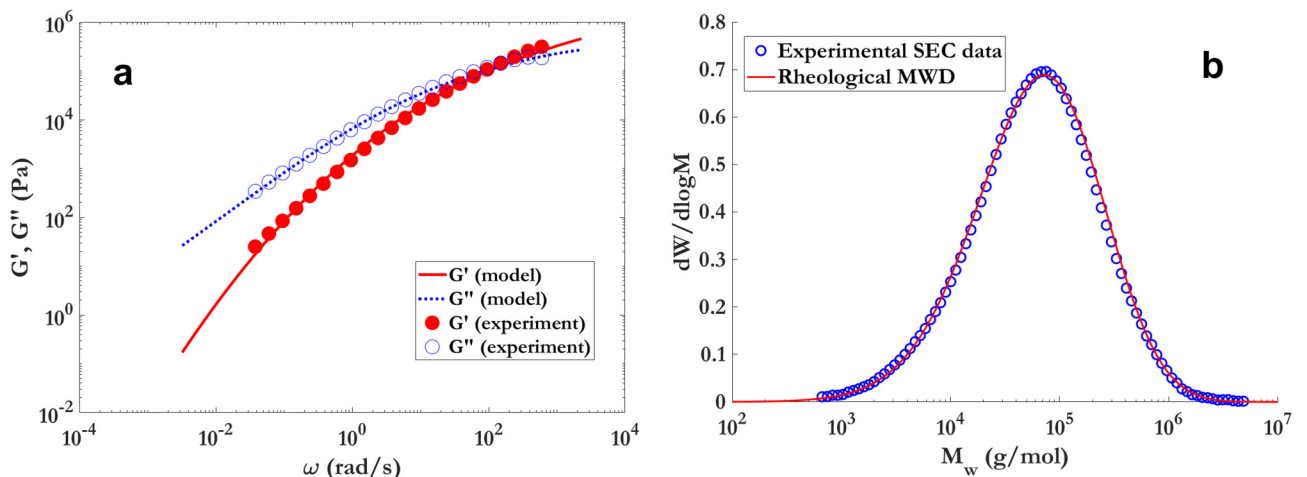


FIG. 7. Results of fitting the TDD-DR + GEX model to the SAOS data of HDPE used in this work. (a) Fitting the model to SAOS data by keeping M^* the same as that for dPE and (b) resultant MWD obtained from the inversion algorithm compared against experimental SEC data.

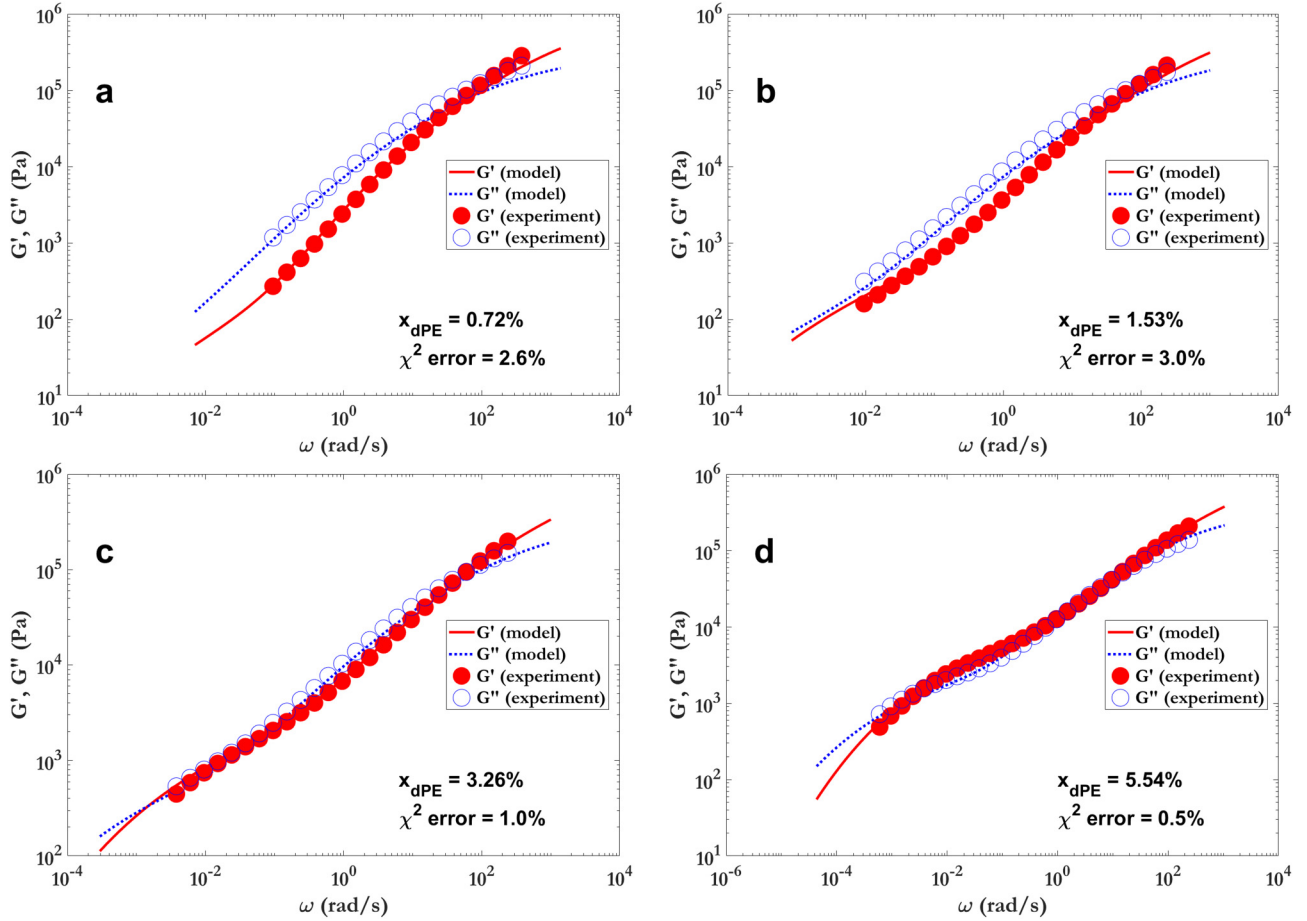


FIG. 8. Comparison of fits of the TDD-DR model for bimodal blends with SAOS data for dPE/HDPE blends of (a) 1%, (b) 2%, (c) 5%, and (d) 10% dPE by weight. χ^2 values are indicated in the figures. The calculated extent of dissolution of dPE x_{dPE} in each blend is also indicated in the figures.

molecular weight distributions $w_{dPE}(M)$ and $w_{HDPE}(M)$ were taken as their respective GEX representations using a , b , and M_0 values in Table I. The relaxation functions $\mu_{d,dPE}(t, M)$ and $\mu_{d,HDPE}(t, M)$ were calculated from Eqs. (1)–(4) using K and M^* values listed in Table I. Starting from an initial guess value of x_{dPE} , the relaxation modulus of the blend was calculated from Eq. (7). This was then Fourier transformed to give $G'_{blend}(\omega)$ and $G''_{blend}(\omega)$, which were compared with experimental SAOS data of the blend to get a revised value of x_{dPE} . This iterative fitting procedure was repeated until converged values of x_{dPE} were obtained as per the criterion mentioned in Eq. (11).

The results of fitting Eq. (7) with experimental data are shown in Fig. 8 for all the blends prepared in this work. As is evident from Fig. 8, good fits were obtained between experimental data and the theoretical model over the entire frequency range used in the experiments for all blends with one unique x_{dPE} value for each blend. Features such as multiple crossover points were also reproduced well by the theory. The goodness of the model fit as indicated by χ^2 values ranging from 0.5% to 3.0% validates the quadratic mixing rule given by the DR theory. Following van Ruymbeke *et al.* [34], the option of using the same value of K (and M^*) or the two individual polymers dPE and HDPE was also exercised in Eq. (7). The results are shown in Fig. S1 of the supplementary material [56]. It was observed that the quality of

model fit to the experimental SAOS data of dPE/HDPE blends was poorer when both parameters were kept identical for the two polymers than when K was allowed to be different. Hence, the values of parameters listed in Table I were preferred in this work.

The predicted values for the dissolved amounts of dPE in each blend are summarized in Table II and also shown in Fig. 9. This is the first time that the actual amounts of dissolved UHMWPE in blends of dPE/HDPE have been calculated. The amount of dPE dissolved in the blend (x_{dPE}) is seen to increase with an increasing amount of dPE added to the blend. However, the difference between dPE dissolved and dPE added increased with an increasing amount of dPE added. Yet, it is encouraging to see that 50–70% of the dPE

TABLE II. Comparison of the amount of dPE added to melt compounder versus the amount of dissolved dPE (x_{dPE}) obtained from fitting Fourier transform of Eq. (7) to experimental SAOS data of blends.

| Name of sample | wt. % of dPE added to blend | wt. % of dPE dissolved in blend (x_{dPE}) | χ^2 error |
|----------------|-----------------------------|---|----------------|
| 1_dPE | 1 | 0.718 | 0.025 |
| 2_dPE | 2 | 1.533 | 0.0297 |
| 5_dPE | 5 | 3.257 | 0.0099 |
| 10_dPE | 10 | 5.539 | 0.0049 |

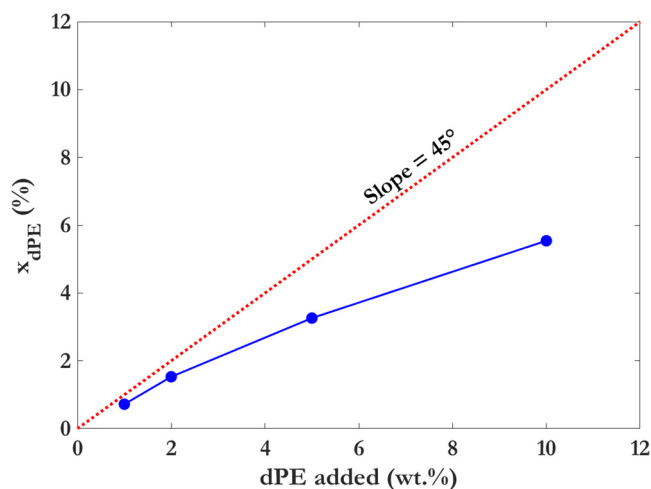


FIG. 9. Comparison of the amount of dPE dissolved in dPE/HDPE blends during melt compounding with the amount of dPE added initially. Comparison with the 45° dashed line indicates that the extent of dissolution of dPE does not increase proportionally with the quantity added.

added during melt compounding had actually dissolved in the blend over a mixing time of as low as 5 min and at a reasonable screw speed of 150 rpm. This suggests that true bimodal blends of polyethylene, in which the MWDs of the two pure components are well separated, can be prepared by melt compounding route. Quantification of the dissolved amount of dPE can help in further optimization of compounding parameters and screw geometry.

V. CONCLUSIONS

In this paper, we have shown that the extent of dissolution of UHMWPE in melt compounded HDPE/UHMWPE blends can be quantified by fitting rheological models of bimodal blends of polydisperse polymers to linear viscoelastic data of these blends. This is perhaps the only way to determine how much of UHMWPE added to HDPE during melt compounding has actually dissolved to create a molecularly mixed entangled blend. The UHMWPE used in this work is a disentangled polymer before melt-mixing. During compounding, a part of it dissolves and entangles with HDPE. The resultant blends, especially those containing higher loading of the UHMWPE, showed complex linear viscoelastic behavior with multiple crossover points and nonmonotonic $\tan \delta$ in the frequency sweep data.

The rheological model of bimodal blends is based on a quadratic mixing rule that accounts for binary interactions between long and short chains of the blend as dictated by des Cloizeaux's DR theory. The model requires information on MWD of individual homopolymers. While the MWD for HDPE was independently measured using HT-SEC, the MWD of UHMWPE was obtained from the rheological method that involved inversion of the stress relaxation function derived from des Cloizeaux's TDD model coupled with the DR theory and a GEX function to describe the MWD. A robust inversion algorithm was developed in MATLAB. Five model parameters were required to be determined simultaneously during inversion. The intrinsic ill-posed nature of the

mathematical problem implies that the choice of initial guess values of the parameters is important. In the present work, the choices for initial guess values were guided partly by the literature and partly by the physical meaningfulness of the results. The inversion algorithm was first validated on a couple of UHMWPE samples for which linear viscoelastic data, as well as HT-SEC data, are available in the literature. An excellent match was obtained between rheologically determined MWD and HT-SEC data for these samples. The algorithm was then used to determine the MWD of the UHMWPE samples used in this work. Having thus obtained the MWD for both homopolymers, the model of bimodal blends now has only one unknown parameter, namely, the fraction of dissolved UHMWPE. This was determined by fitting the model to experimental linear viscoelasticity data of blends. With a single value of this parameter for each blend, the model was able to provide a good fit to the data over the measured frequency range.

It was found that nearly 50–70 wt. % of the UHMWPE could be dissolved in HDPE during melt compounding. This is a significant degree of dissolution considering that the residence time used in melt-mixing was only ~5 min. The methodology developed in this work to determine the extent of dissolution is expected to be useful while developing bimodal grades of polymers by the melt compounding route. The methodology will also be useful in determining the kinetics of dissolution of dPE in HDPE, the physics of which is likely to involve the following steps: (i) melting of single crystals of dPE and accompanying “explosion” of R_g [54], (ii) interpenetration of dPE chains with HDPE at the surface of the dPE particles [55], and (iii) center-of-mass motion of dPE chains due to convection (such as in a micro-compounder) or by diffusion in the quiescent state (such as in a rheometer).

ACKNOWLEDGMENTS

K.C. is grateful for receiving a doctoral research fellowship from Reliance Industries Ltd. The authors are grateful to Professor Sanjay Rastogi and Reliance Industries Ltd for the generous supply of the dPE and HDPE samples, respectively.

REFERENCES

- [1] DesLauriers, P. J., M. P. McDaniel, D. C. Rohlfing, R. K. Krishnaswamy, S. J. Secora, E. A. Benham, P. L. Maeger, A. R. Wolfe, A. M. Sukhadia, and B. B. Beaulieu, “A comparative study of multimodal vs bimodal polyethylene pipe resins for PE-100 applications,” *Polym. Eng. Sci.* **45**, 1203–1213 (2005).
- [2] Zuo, J., Y. M. Zhu, S. M. Liu, Z. J. Jiang, and J. Q. Zhao, “Preparation of HDPE/UHMWPE/MMWPE blends by two-step processing way and properties of blown films,” *Polym. Bull.* **58**, 711–722 (2007).
- [3] Rezaei, M., N. G. Ebrahimi, and M. Kontopoulou, “Thermal properties, rheology and sintering of ultra high molecular weight polyethylene and its composites with polyethylene terephthalate,” *Polym. Eng. Sci.* **45**, 678–686 (2005).
- [4] Bhateja, S. K., and E. H. Andrews, “Thermal, mechanical, and rheological behavior of blends of ultrahigh and normal-molecular-weight linear polyethylenes,” *Polym. Eng. Sci.* **23**, 888–894 (1983).

- [5] Vadhar, P., and T. Kyu, "Effects of mixing on morphology, rheology, and mechanical properties of blends of ultra-high molecular weight polyethylene with linear low-density polyethylene," *Polym. Eng. Sci.* **27**, 202–210 (1987).
- [6] Kyu, T., and P. Vadhar, "Cocrystallization and miscibility studies of blends of ultrahigh molecular weight polyethylene with conventional polyethylenes," *J. Appl. Polym. Sci.* **32**, 5575–5584 (1986).
- [7] Boscoletto, A. B., R. Franco, M. Scapin, and M. Tavan, "An investigation on rheological and impact behaviour of high density and ultra high molecular weight polyethylene mixtures," *Eur. Polym. J.* **33**, 97–105 (1997).
- [8] Ruff, M., and C. Paulik, "Controlling polyolefin properties by In-reactor blending, 1-polymerization process, precise kinetics, and molecular properties of UHMW-PE polymers," *Macromol. React. Eng.* **6**, 302–317 (2012).
- [9] Ruff, M., and C. Paulik, "Controlling polyolefin properties by In-reactor blending: 2. Particle design," *Macromol. React. Eng.* **7**, 71–83 (2013).
- [10] Ruff, M., R. W. Lang, and C. Paulik, "Controlling polyolefin properties by in-reactor blending: 3. Mechanical properties," *Macromol. React. Eng.* **7**, 328–343 (2013).
- [11] Dumoun, M. M., L. A. Utracki, and J. Lara, "Rheological and mechanical behavior of the UHMWPE/MDPE mixtures," *Polym. Eng. Sci.* **24**, 117–126 (1984).
- [12] Tinçer, T., and M. Coşkun, "Melt blending of ultra high molecular weight and high density polyethylene: The effect of mixing rate on thermal, mechanical, and morphological properties," *Polym. Eng. Sci.* **33**, 1243–1250 (1993).
- [13] Pi, L., X. Hu, M. Nie, and Q. Wang, "Role of ultrahigh molecular weight polyethylene during rotation extrusion of polyethylene pipe," *Ind. Eng. Chem. Res.* **53**, 13828–13832 (2014).
- [14] Xu, L., C. Chen, G.-J. Zhong, J. Lei, J.-Z. Xu, B. S. Hsiao, and Z.-M. Li, "Tuning the superstructure of ultrahigh-molecular-weight polyethylene/low-molecular-weight polyethylene blend for artificial joint application," *ACS Appl. Mater. Interfaces* **4**, 1521–1529 (2012).
- [15] Diop, M. F., W. R. Burghardt, and J. M. Torkelson, "Well-mixed blends of HDPE and ultrahigh molecular weight polyethylene with major improvements in impact strength achieved via solid-state shear pulverization," *Polymer* **55**, 4948–4958 (2014).
- [16] Chaudhuri, K., S. Poddar, H. Pol, A. Lele, A. Mathur, G. S. Srinivasa Rao, and R. Jasra, "The effect of processing conditions on the rheological properties of blends of ultra high molecular weight polyethylene with high-density polyethylene," *Polym. Eng. Sci.* **59**, 821–829 (2019).
- [17] Yang, H., L. Hui, J. Zhang, P. Chen, and W. Li, "Effect of entangled state of nascent UHMWPE on structural and mechanical properties of HDPE/UHMWPE blends," *J. Appl. Polym. Sci.* **134**, 1–8 (2017).
- [18] Talebi, S., R. Duchateau, S. Rastogi, J. Kaschta, G. W. M. Peters, and P. J. Lemstra, "Molar mass and molecular weight distribution determination of UHMWPE synthesized using a living homogeneous catalyst," *Macromolecules* **43**, 2780–2788 (2010).
- [19] Rastogi, S., L. Kurelec, J. Cuijpers, D. R. Lippits, M. Wimmer, and P. J. Lemstra, "Disentangled state in polymer melts; a route to ultimate physical and mechanical properties," *Macromol. Mater. Eng.* **288**, 964–970 (2003).
- [20] Lippits, D. R., S. Rastogi, S. Talebi, and C. Bailly, "Formation of entanglements in initially disentangled polymer melts," *Macromolecules* **39**, 8882–8885 (2006).
- [21] Pandey, A., Y. Champouret, and S. Rastogi, "Heterogeneity in the distribution of entanglement density during polymerization in disentangled ultrahigh molecular weight polyethylene," *Macromolecules* **44**, 4952–4960 (2011).
- [22] Ronca, S., G. Forte, H. Tjaden, Y. Yao, and S. Rastogi, "Tailoring molecular structure via nanoparticles for solvent-free processing of ultra-high molecular weight polyethylene composites," *Polymer* **53**, 2897–2907 (2012).
- [23] Romano, D., S. Ronca, and S. Rastogi, "A hemi-metallocene chromium catalyst with trimethylaluminum-free methylaluminoxane for the synthesis of disentangled ultra-high molecular weight polyethylene," *Macromol. Rapid Commun.* **36**, 327–331 (2015).
- [24] Pandey, A., A. Toda, and S. Rastogi, "Influence of amorphous component on melting of semicrystalline polymers," *Macromolecules* **44**, 8042–8055 (2011).
- [25] Gennes, P.-G., *Scaling Concepts in Polymer Physics* (Cornell University, Ithaca, 1979).
- [26] de Gennes, P. G., "Reptation of a polymer chain in the presence of fixed obstacles," *J. Chem. Phys.* **55**, 572–579 (1971).
- [27] Doi, M., and S. F. Edwards, *The Theory of Polymer Dynamics* (Oxford University, Oxford, 1988).
- [28] Rubinstein, M., and R. H. Colby, "Self-consistent theory of polydisperse entangled polymers: Linear viscoelasticity of binary blends," *J. Chem. Phys.* **89**, 5291–5306 (1988).
- [29] des Cloizeaux, J., "Relaxation and viscosity anomaly of melts made of long entangled polymers: Time-dependent reptation," *Macromolecules* **23**, 4678–4687 (1990).
- [30] des Cloizeaux, J., "Polymer melts: A theoretical justification of double reptation," *J. Phys.* **13**, 61–68 (1993).
- [31] Mead, D. W., "Component predictions and the relaxation spectrum of the double reptation mixing rule for polydisperse linear flexible polymers," *J. Rheol.* **40**, 633–661 (1996).
- [32] des Cloizeaux, J., "Double reptation vs simple reptation in polymer melts," *Europhys. Lett.* **5**, 437–442 (1988).
- [33] des Cloizeaux, J., "Relaxation of entangled and partially entangled polymers in melts: Time-dependent reptation," *Macromolecules* **25**, 835–841 (1992).
- [34] van Ruymbeke, E., R. Keunings, V. Stéphenne, A. Hagenaars, and C. Bailly, "Evaluation of reptation models for predicting the linear viscoelastic properties of entangled linear polymers," *Macromolecules* **35**, 2689–2699 (2002).
- [35] van Ruymbeke, E., R. Keunings, and C. Bailly, "Determination of the molecular weight distribution of entangled linear polymers from linear viscoelasticity data," *J. Nonnewton. Fluid Mech.* **105**, 153–175 (2002).
- [36] Doi, M., "Explanation for the 3.4-power law for viscosity of polymeric liquids on the basis of the tube model," *J. Polym. Sci. Polym. Phys. Ed.* **21**, 667–684 (1983).
- [37] Larson, R. G., T. Sridhar, L. G. Leal, G. H. McKinley, A. E. Likhtman, and T. C. B. McLeish, "Definitions of entanglement spacing and time constants in the tube model," *J. Rheol.* **47**, 809–818 (2003).
- [38] Colby, R. H., L. J. Fetters, and W. W. Graessley, "The melt viscosity-molecular weight relationship for linear polymers," *Macromolecules* **20**, 2226–2237 (1987).
- [39] Fetters, L. J., D. J. Lohse, and R. H. Colby, Chain dimensions and entanglement spacings, in *Physical Properties of Polymers Handbook* (Springer, New York, 2007).
- [40] Tsenoglou, C., "Molecular weight polydispersity effects on the viscoelasticity of entangled linear polymers," *Macromolecules* **24**, 1762–1767 (1991).
- [41] Tsenoglou, C., "Viscoelasticity of binary polymer blends," *ACS Polym. Prepr.* **28**, 185–186 (1987).
- [42] Jam, J. E., M. Nekoomanesh, M. Ahmadi, and H. Arabi, "From molecular weight distribution to linear viscoelastic properties and back again:

- Application to some commercial high-density polyethylenes,” *Iran. Polym. J.* **21**, 403–413 (2012).
- [43] Zulli, F., M. Giordano, and L. Androzzi, “Onset of entanglement and reptation in melts of linear homopolymers: Consistent rheological simulations of experiments from oligomers to high polymers,” *Rheol. Acta* **54**, 185–205 (2015).
- [44] Léonardi, F., J.-C. Majesté, A. Allal, and G. Marin, “Rheological models based on the double reptation mixing rule: The effects of a polydisperse environment,” *J. Rheol.* **44**, 675–692 (2000).
- [45] Carrot, C., and J. Guillet, “From dynamic moduli to molecular weight distribution: A study of various polydisperse linear polymers,” *J. Rheol.* **41**, 1203–1220 (1997).
- [46] Nobile, M. R., and F. Cocchini, “Evaluation of molecular weight distribution from dynamic moduli,” *Rheol. Acta* **40**, 111–119 (2001).
- [47] Guzmán, J. D., J. D. Schieber, and R. Pollard, “A regularization-free method for the calculation of molecular weight distributions from dynamic moduli data,” *Rheol. Acta* **44**, 342–351 (2005).
- [48] Ferry, J. D., *Viscoelastic Properties of Polymers* (Wiley, New York, 1980), pp. 81.
- [49] Schwarzl, F. R., “Numerical calculation of storage and loss modulus from stress relaxation data for linear viscoelastic materials,” *Rheol. Acta* **10**, 165–173 (1971).
- [50] Nelder, J. A., and R. Mead, “A simplex method for function minimization,” *Comput. J.* **7**, 308–313 (1965).
- [51] Mead, D. W., “Determination of molecular weight distributions of linear flexible polymers from linear viscoelastic material functions,” *J. Rheol.* **38**, 1797 (1994).
- [52] Liu, C., J. He, E. van Ruymbeke, R. Keunings, and C. Bailly, “Evaluation of different methods for the determination of the plateau modulus and the entanglement molecular weight,” *Polymer* **47**, 4461–4479 (2006).
- [53] van Ruymbeke, E., C. Liu, and C. Bailly, “Quantitative tube model predictions for the linear viscoelasticity of linear polymers,” *Rheol. Rev.* **2007**, 53–134 (2007).
- [54] Barham, P. J., and D. M. Sadler, “A neutron scattering study of the melting behaviour of polyethylene single crystals,” *Polymer* **32**, 393–395 (1991).
- [55] Xue, Y.-Q., T. A. Tervoort, and P. J. Lemstra, “Welding behavior of semicrystalline polymers. 1. The effect of nonequilibrium chain conformations on autoadhesion of UHMWPE,” *Macromolecules* **31**, 3075–3080 (1998).
- [56] See supplementary material at <https://doi.org/10.1122/1.5113705> for results of fitting the rheological data of the blends using the method of van Ruymbeke *et al.* [34], keeping the TDD-DR parameters constant between PE components.